AEDC-TR-69-32

ey'

A MULTIMODED CAVITY PROBE TO PROVIDE HIGH SPATIAL RESOLUTION OF WAKE TRAIL IONIZATION MEASUREMENT

D. Rosenberg

Electrical Engineering Department

The University of Tennessee
Knoxville, Tennessee

February 1969

ARNOLD ENGINEERING DEVELOPMENT CENTER

AIR FORCE SYSTEMS COMMAND

ARNOLD AIR FORCE STATION, TENNESSEE

NOTICES

A MULTIMODED CAVITY PROBE TO PROVIDE HIGH SPATIAL

RESOLUTION OF WAKE TRAIL IONIZATION MEASUREMENT

D. Rosenberg
Electrical Engineering Department
The University of Tennessee
Knoxville, Tennessee

FOREWORD

The reproducibles used in the reproduction of this report were
supplied by the author.

This technical report has been reviewed and is approved.

Marshall K. Kingery
Research Division
Directorate of Plans
and Technology

Edward R. Feicht
Colonel, USAF
Director of Plans
and Technology

ABSTRACT

This report discusses properties and use of a highly resolving
r.f. cavity probe system for wake trails in hypervelocity model ranges.
Data are taken from two distinct modes of the system and yield electric
susceptance at an average axial position inside the cavity. This is
important in wake trail study, since it ties together a wake electrical
measurement with distance behind a hypervelocity model.

CONTENTS

ILLUSTRATIONS

TABLES

NOMENCLATURE

a	unsubscripted, wake radius
a_{ij}	subscripted, matrix element
b	unsubscripted, cavity radius
b_{ij}	subscripted, matrix element
d = e + f	cavity length in terms of rearward e and forward f division.
$\mathbf{E}$, E	electric field vector and scalar component
h	propagation constant
$\mathbf{H}$, H	magnetic field vector and scalar component
k	wavenumber
K-1	susceptibility in e
$\overline{K-1}$	averaged susceptibility in d = e + f
M-1	susceptibility in f
q	normalized Q factor
Q	circuit Q factor
r, $\hat{r}$	radial coordinate and unit vector
$s = \sigma + j\omega$	complex radian frequency ω and decay rate
TM_{mn}, TM_{mnl}	respectively waveguide and cavity TM waves
x	variable
$y = g + j(\omega C - \frac{1}{\omega L})$	normalized admittance in Section II
y	variable in Appendix A
z, $\hat{z}$	longitudinal coordinate and unit vector

γ propagation constant

Δ unsubscripted, increment

Δ_{ij} subscripted, inner product of unit Bessel functions $\psi_i \psi_j$

λ eigenvalue

$\boldsymbol{\pi}, \pi$ vector potential and scalar component

σ time decay rate

Φ radial component of potential

ψ unit Bessel function, $\|\psi_i\| = 1$

Ψ longitudinal component of potential

ω radian frequency

SECTION I
INTRODUCTORY REMARKS

This final report discusses properties and use of a highly resolving r.f. cavity probe system for hypervelocity wake trails. Data are taken from two distinct modes of the system and yield electric susceptance at an average axial position inside the cavity. These are important data in wake trail study, since they tie wake electrical measurement together with distance behind a hypervelocity model. Below, following brief description of a current trend in wake trail study, the basic probe system will be indicated, and an outline made of subsequent consideration of design problems of the multimoded probe.

Shock dominated wakes of blunt bodies in air are characterized by rapid decay of large initial ionization. Decay is more rapid as ambient pressure increases, and ionization is quenched by the nearly complete reaction of ablated material with air -- when ablation is present -- and reassociation of air components. A rough picture of the reacting sequence (following Kornegay, Ref. 8) is given at least in the following steps: electron dissociation in air, electron association with oxygen, completed by ionized oxygen attachment to positive ions. The data of Kornegay are similar, except for ionization level, to the data of Hendrix and Mayfield.

The process can be seeded, most likely by ablated material or

1

by contaminants of air. It is known, for example, that traces of sodium
in air can contribute significantly to electron population and to collision
frequency because of extremely low ionization potential (Refs. 2 and 6).
Such behaviour of contaminants provides sources of electrons to speed
the pure air reactions. However, it appears that data on initiation
of ionization for these chemical processes, and on the role of air
contaminants therein, have not much been measured.

In all, air is a complicated substance. Its properties are often
better measured experimentally than predicted theoretically. It is the
purpose of this report to describe characteristics of a wake trail
measuring system (a multiple moded r.f. cavity) which retains two useful
properties in its measurements: namely, continuousness and high resolution
of data, axially along the wake trail. In a sense, the system is a
prototype. It could also yield resolved radial data.

A primitive block diagram for the system is shown in Figure 1.
There are other approaches to the measurement, of which this is the
simplest one. For definiteness, it is assumed excited in the TM_{020}
mode with output by the TM_{011} mode. After calibrating without the
wake, only two readings are needed when the wake is present, the
reflection and transmission coefficients or equivalents. The amplifier
inserted in the output side will help accuracy of the measurement.
Accuracy is best when input and output both are read at about the same
level. The degree of accuracy in the design calculations done here
can be illustrated by an example. If wake Q is about 100 (exaggerated),

2

then the system will yield a complex dielectric constant, averaged only radially, at a point inside a 0.1 inch interval of a 10 inch long cavity.
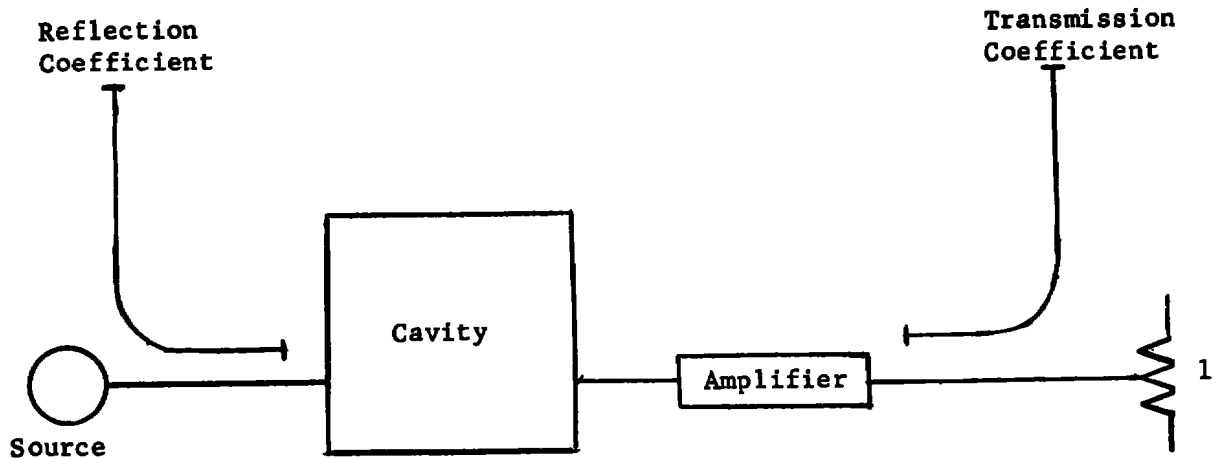
Fig. 1 System Block Diagram

It is well to point out that multimoding the system requires only that reading be done on two different modes. It is not necessary that these be simultaneously resonant. It is merely convenient. It can retain small size of equipment when modes resonate together. There is however a maximum of three modes that can resonate at once in the cavity. Thus a higher moded system would use separate cavities or separate frequencies to operate. The choice can be one of practical convenience. What is necessary for system operation, however, is just measurement on distinct* modes.

---

*Even this is not unqualified. The same modes in different size cavities could also yield a reading of wake susceptance.

3

Material discussed subsequently is, in outline, as follows.
Section II will present the system equivalent circuits and consider
the relation of circuit resonances with measured circuit parameters.
Results are shown in Table II. In Section III, by solving electro-
magnetic field equations, circuit resonances and measured parameters
are related to cavity and wake physical properties. These results
are shown in Table VII. The interesting question of optimizing the
wake measurement is considered in Section IV. One is asked, equiva-
lently, to measure the wake inside the cavity at an axial position
that divides the weight of ions in half. These results, in Table
VIII, locate the wake average susceptance at its average position
inside the cavity. An appendix discusses error (the largest one)
in solving the field equations in Section III.

SECTION II
PERTURBED CAVITY EQUIVALENT CIRCUIT PARAMETERS

The cavity can be viewed as a network nested inside another network called the internal circuit. This is shown in Figure 2. Whatever attaches to the ports of the internal circuit, one can call the external circuit. An ordinary analysis would determine properties of the cavity by solving an electromagnetic boundary value problem, but neglecting wall losses. Wall losses are then usually either easily measured or else easily calculated from the now known lossless wall solution. All this would determine the elements of the internal circuit of Figure 2. The unit conductances represent cavity wall losses.

In case the cavity is loaded with a slightly lossy filling, then the lossless solution can be made to serve here also. This is true even when variational approaches are taken, so long as system Q factors are high, as they are assumed to be for the present cavity. All the above mentioned procedural steps, will be taken in considering this design of a two moded cavity. However, the present section will focus on behaviour of the circuit needed to represent the system.

An extended analysis would account also for the coupling circuits to the cavity, but these additional loadings are ineffective for the most part, and are overlooked therefore. They could be considered separately. Sources to drive the cavity and meters to measure transmissions

5

External
Circuit

External
Circuit

Y_E 1   Cavity   1 Y_E

Side 1
TM_{020}

Side 2
TM_{011}
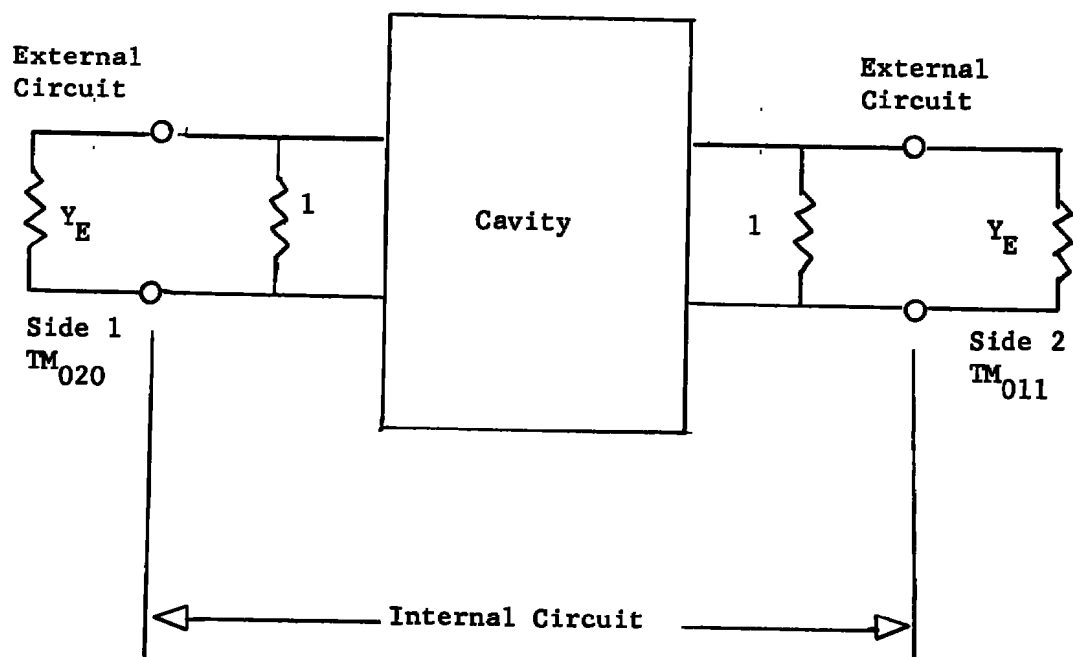
Internal Circuit

Fig. 2 Internal and External Circuits

and reflections are located in the external circuit. In order that

sources and metering equipment not contribute reflections to the system,

beyond those due only to the internal circuit, external circuits are

assumed adjustable to match with g = 1.

The cavity circuit exists in two states, measurements on both

of which are required in order to characterize the wake. The state

shown in Figure 3(a) occurs for the empty cavity. In this state, the

circuit parameters L_o, C_o, the double resonance measurement frequency

$$\omega_o^2 = \frac{1}{\sqrt{L_o C_o}} \qquad , \qquad \text{---(1)}$$

and the numbers q_o and q can all be found or measured. Here,

$$q_o = \frac{Q_2}{Q_1} \qquad \text{---(2)}$$

is the ratio of internal circuit Q's (TM_{011} to TM_{020}) of the empty

waveguide, while

$$q = q_o \left(\frac{k_2}{k_1} \right) \qquad , \qquad \text{---(2a)}$$

where k_1 and k_2 are wave numbers respectively for TM_{02} and TM_{01} circular

waveguide modes.

In its second state, that shown in Figure 3(b), the cavity holds

a model wake. It is here that results of an electromagnetic boundary

value problem will be used to relate to circuit parameters. However, the

7
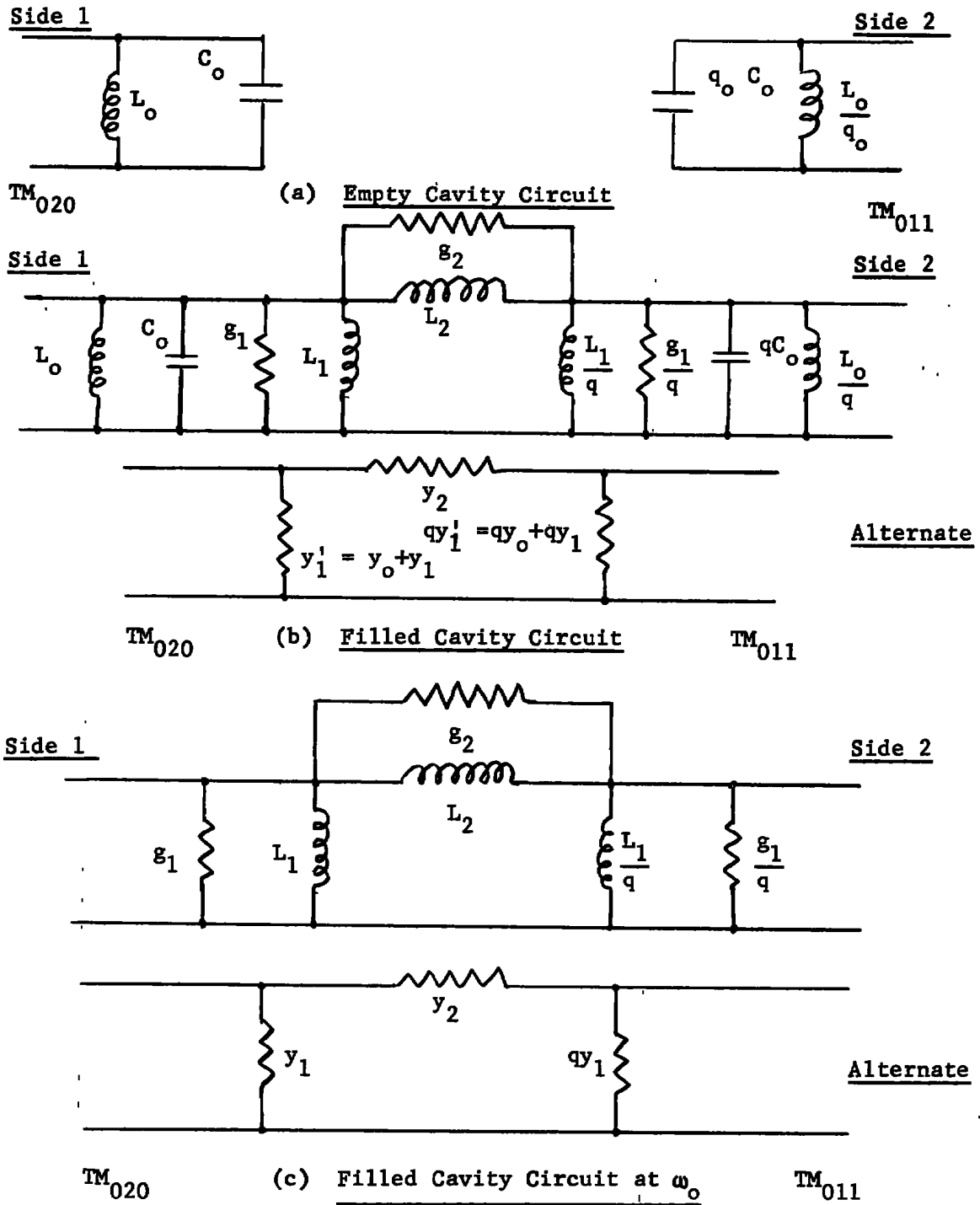
Fig. 3 States of the Cavity Circuit

wake is present for only a few hundred microseconds and this means there is no time to check out completely the Figure 3(b) circuit (against frequency). Instead, a quick measurement is made on the circuit in Figure 3(c). By inference, this is related to the Figure 3(b) circuit from results of the solved electromagnetic field equations. The Figure 3(a) circuit, the first state, having been checked out before the model flight, then all parameters in the equivalent cavity circuit therefore would have become measured.

The cavity circuit admittance, when the wake is present, has two zero resonance conditions,

$$y_1' = 0 \qquad\qquad\qquad \text{---(3)}$$

and

$$qy_1' + (1 + q)y_2 = 0 \qquad , \qquad\qquad \text{---(4)}$$

whether looking in at Side 1 (TM_{020} terminals) or at Side 2 (TM_{011} terminals). This reflects the property of the wake that it does not merely shift the individual modal frequencies, but rather it couples them together making resonances such that the modes are jointly present. The fact that the same split and shift in resonance occurs at Side 1 as at Side 2 follows from solution of the field equations.[*]

---

[*]It is the same effect that causes the change of q_o to q between the Figure 3(a) and the 3(b) and 3(c) circuits. It is due to the fact that cavity magnetizing current transfers from terminals 1 to 2 by the real number factor $\left(\dfrac{k_1}{k_2}\right)^2$ different from the transfer from terminals 2 back to 1.

By contrast, since the cavity circuit of Figure 3(b) is not symmetrical, the admittance pole resonances are not constrained to be the same at both terminals. Here, the pole resonance condition on Side 1 is that

$$qy_1' + y_2 = 0 \qquad , \qquad\qquad\qquad ---(5)$$

and on Side 2 it is that

$$y_1' + y_2 = 0 \qquad . \qquad\qquad\qquad ---(6)$$

All these relations, (1) through (6), used with the cavity circuit parameters shown in Figure 3, will yield the s-plane resonances listed in Table I. The numbers $s = \sigma + j\omega$ correspond to resonant frequencies ω and to time decay rates σ due to losses in the cavity circuit. Because the circuit is very high Q ($\gg 100$), the frequencies ω are approximately the same as they would be for a lossless cavity and lossless wake.

The Table I. formulary can be used to obtain expressions for the circuit elements explicitly in terms of the resonant decay rates and frequencies. These are listed in Table II. They are important, on the one hand, in relating measured circuit parameters with calculated fre-quencies and decay rates. On the other hand, the several Q formulas listed are design criteria for the system in that these numbers reflect the manner of shifts of admittance zeroes under loading of the cavity. Thus,

10

TABLE I

CAVITY RESONANCES

Admittance
Resonances

$$s = \sigma + j\omega$$

Empty Cavity

$$\omega_o = \frac{1}{\sqrt{C_o L_o}} \quad , \text{ The Measuring Frequency}$$

Low Zero

$$s_1 = \sigma_1 + j\omega_1 = -\frac{g_1}{2C_o} + j\sqrt{\frac{1}{C_o}\left(\frac{1}{L_o} + \frac{1}{L_1}\right)}$$

Side 1 Pole
TM_{020} Terminals

$$s_{21} = \sigma_{21} + j\omega_{21}$$

$$= \frac{-1}{2C_o}\left(g_1 + \frac{1}{q}g_2\right) + j\sqrt{\frac{1}{C_o}\left(\frac{1}{L_o} + \frac{1}{L_1} + \frac{1}{q}\frac{1}{L_2}\right)}$$

Side 2 Pole
TM_{011} Terminals

$$s_{22} = \sigma_{22} + j\omega_{22}$$

$$= \frac{-1}{2C_o}\left(g_1 + g_2\right) + j\sqrt{\frac{1}{C_o}\left(\frac{1}{L_o} + \frac{1}{L_1} + \frac{1}{L_2}\right)}$$

High Zero

$$s_3 = \sigma_3 + j\omega_3$$

$$= \frac{-1}{2C_o}\left[g_1 + \left(1 + \frac{1}{q}\right)g_2\right] + j\sqrt{\frac{1}{C_o}\left[\frac{1}{L_o} + \frac{1}{L_1} + \left(1 + \frac{1}{q}\right)\frac{1}{L_2}\right]}$$

$$\omega_o \leqslant \omega_1 \leqslant \omega_{21}, \omega_{22} \leqslant \omega_3$$

$$0 < \sigma_1 \leqslant \sigma_{21}, \sigma_{22} \leqslant \sigma_3$$

INTERRELATIONS

$$\left(1 + \frac{1}{q}\right)\omega_{22}^2 = \omega_3^2 + \frac{1}{q}\omega_1^2 \text{ and } (1 + q)\omega_{21}^2 = \omega_3^2 + q\omega_1^2$$

$$\left(1 + \frac{1}{q}\right)\sigma_{22} = \sigma_3 + \frac{1}{q}\sigma_1 \text{ and } (1 + q)\sigma_{21} = \sigma_3 + q\sigma_1$$

$$\omega_{22}^2 + \omega_{21}^2 = \omega_3^2 + \omega_1^2 \text{ and } (1 + q)(\omega_{22}^2 - \omega_{21}^2) = (q - 1)(\omega_3^2 - \omega_1^2)$$

$$\sigma_{22} + \sigma_{21} = \sigma_3 + \sigma_1 \text{ and } (1 + q)(\sigma_{22} - \sigma_{21}) = (q - 1)(\sigma_3 - \sigma_1)$$

11

TABLE II
MEASUREMENT AND DESIGN RELATIONS

$$q = \frac{k_2 Q_2}{k_1 Q_1}$$

Measurement Formulas

$$\frac{\omega_1^2 - \omega_o^2}{\omega_o^2} = \frac{L_o}{L_1}$$

$$\frac{-2\sigma_1}{\omega_o} = \frac{g_1}{Q_1}$$

$$\frac{\omega_3^2 - \omega_o^2}{\omega_o^2} = \frac{L_o}{L_1} + (1 + \frac{1}{q}) \frac{L_o}{L_2}$$

$$\frac{-2\sigma_3}{\omega_o} = \frac{1}{Q_1} \left[g_1 + (1 + \frac{1}{q}) g_2 \right]$$

$$\frac{\omega_3^2 - \omega_1^2}{\omega_o^2} = (1 + \frac{1}{q}) \frac{L_o}{L_2}$$

$$\frac{-2(\sigma_3 - \sigma_1)}{\omega_o} = \frac{1}{Q_1} (1 + \frac{1}{q}) g_2$$

Q Formulas

$$\frac{-2\sigma_1 \omega_o}{\omega_1^2 - \omega_1^2} = \omega_o L_1 g_1$$

$$\frac{-2\sigma_3 \omega_o}{\omega_3^2 - \omega_1^2} = \frac{\omega_o L_1 L_2 \left[k_2 Q_2 g_1 + (k_1 Q_1 + k_2 Q_2) g_2 \right]}{k_2 Q_2 L_2 + (k_1 Q_1 + k_2 Q_2) L_1}$$

$$\frac{-2(\sigma_3 - \sigma_1) \omega_o}{\omega_3^2 - \omega_1^2} = \omega_1 L_2 g_2$$

12

for example, it may be necessary to decide whether or not a loaded Q of the order $\frac{Q_1}{10}$ or $\frac{Q_2}{10}$ can yield readable measurements from the system accurately.

Figure 4 illustrates results given in Table I. Cavity and wake are assumed lossless here, so that the graph is one of reactance against frequency, seen from either Side 1 or Side 2 of the cavity. The relative positions of resonances correspond to the Table I listing, and ω_2 is assumed to represent either of the admittance poles ω_{21} or ω_{22}.

The frequencies ω_1 and ω_3 may be characterized very nearly as modal resonances. Strictly speaking, pure TM_{020} and TM_{011} modes are present only in the empty cavity, and are only approximated to in the filled cavity. In particular, the actual fields need to have both modes for components. When the field resonates at ω_1 and ω_3, the TM_{020} and TM_{011} modal components both also resonate, with some coupling between them. When the cavity field resonates at ω_2 (i.e., ω_{21} or ω_{22}) however, neither modal component resonates, but each couples strongly to the other mode. Thus, at ω_{21} for example, if the source is at Side 1, very little energy goes into y_1, but most goes over into y_2 and into qy_1 at Side 2. A similar thing occurs at ω_{22} for a source at Side 2. The frequencies ω_2 are therefore mode conversion resonances. If the TM_{020} terminals are excited, then only a TM_{011} mode appears. If the TM_{011} terminals are excited then only a TM_{020} mode appears. For an input wave of one type, a second wave type is launched.

The measurement frequency ω_o is always below ω_1 for plasmas and

13

$$\omega_o^2 = \frac{1}{L_o C_o}$$

$$\omega_1^2 = \frac{1}{C_o} \left(\frac{1}{L_o} + \frac{1}{L_1}\right)$$
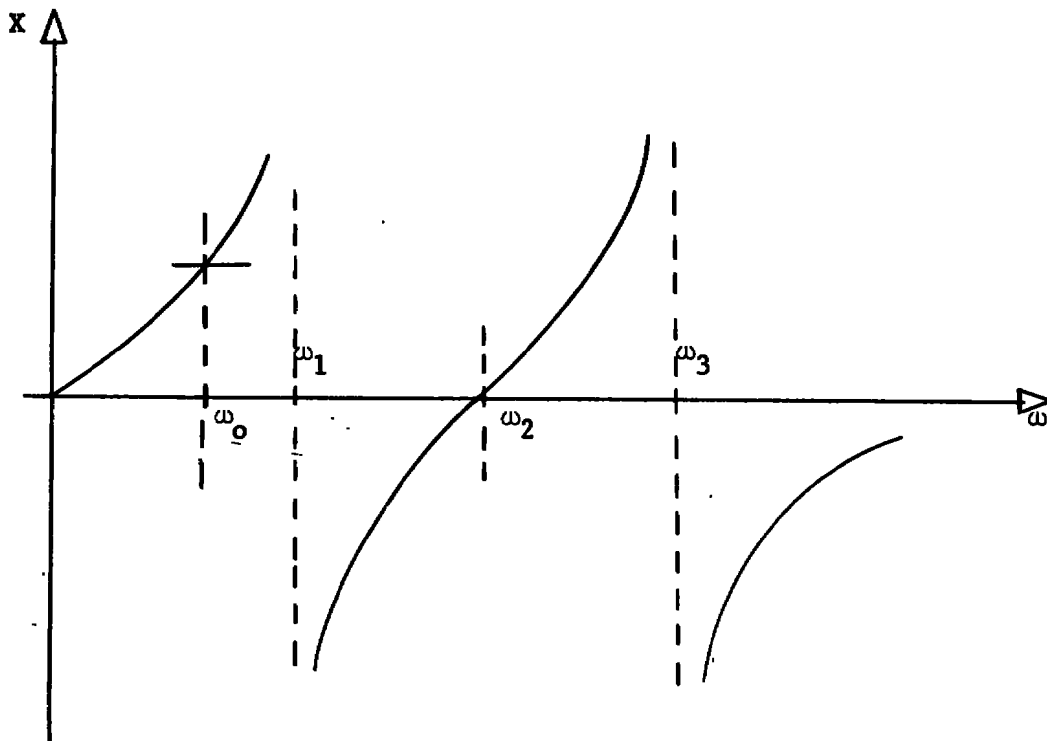
$$\omega_2^2 = \omega_{21}^2 = \frac{1}{C_o} \left(\frac{1}{L_o} + \frac{1}{L_1} + \frac{1}{q}\frac{1}{L_2}\right) \text{at } TM_{020} \text{ terminals}$$

or

$$\omega_2^2 = \omega_{22}^2 = \frac{1}{C_o} \left(\frac{1}{L_o} + \frac{1}{L_1} + \frac{1}{q}\frac{1}{L_2}\right) \text{at } TM_{011} \text{ terminals}$$

$$\omega_3^2 = \frac{1}{C_o} \left[\frac{1}{L_o} + \frac{1}{L_1} + \left(1 + \frac{1}{q}\right)\frac{1}{L_2}\right]$$

Fig. 4 Loaded Cavity Reactance Curve

it is always above ω_3 for non-ionized dielectrics. It could be between ω_1 and ω_3 only if a part of the cavity held a plasma and another part held an ordinary dielectric. This, at the same time, suggests a second picture that can view the mode conversion resonances ω_2. These would be resonances between the forward highly ionized wake and the rearward much decayed wake.

SECTION III
SPLIT AND SHIFTED RESONANCES CALCULATION

Calculation of the resonances $\omega_0 \omega_1 \omega_3$ is done by what can be called a frequency shift method. First, ω_0 will be determined for the empty cavity as a simultaneous resonance of its TM_{011} and TM_{020} modes in terms of cavity dimensions. The frequency of all actual measurement done by the cavity is ω_0. The system will then be perturbed by the wake, and split and shifted resonances $\omega_1 \omega_3$ determined from solving an electromagnetic field boundary value problem. Various generalizations and details of the solution -- by variational technique -- are discussed elsewhere (Refs. 1, 4, and 5). Certain special adjustments to the technique, however, are argued here as the calculation is developed.

The cavity is constructed as shown in Figure 5(a) and is assumed to carry only TM radially symmetric modes. Circular cavity TM wavenumbers are in general found from the relation

$$\left(\frac{p(m,n)}{b}\right)^2 + \left(\frac{l\pi}{d}\right)^2 = k_{oo}^2 \qquad , \qquad \text{---(7)}$$

where b is radius and d is length for the cavity, where $k_{oo}^2 = \omega_o^2 \mu_o \epsilon_o$ is free space wave number at ω_o resonance, and l is an integer. The number $p(m,n)$ is an nth root of an m-order Bessel function, m and n integers. This applies to each mode TM_{mnl}.

16

$$k_2^2 + \left(\frac{\pi}{d}\right)^2 = k_1^2$$

$$k_{oo}b = 5.520$$

$$\frac{b}{d} = 1.585$$

$$\left(\frac{k_1 d}{\pi}\right)^2 = 1.232$$

(a)

(b)
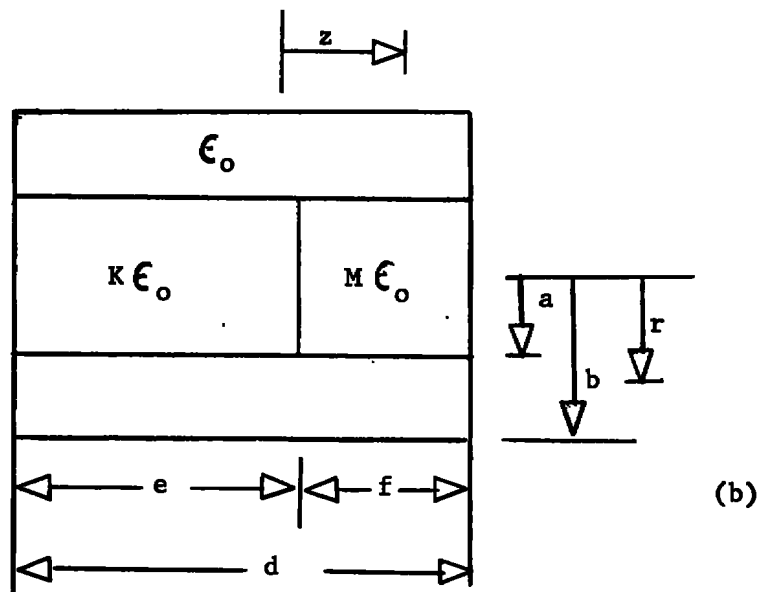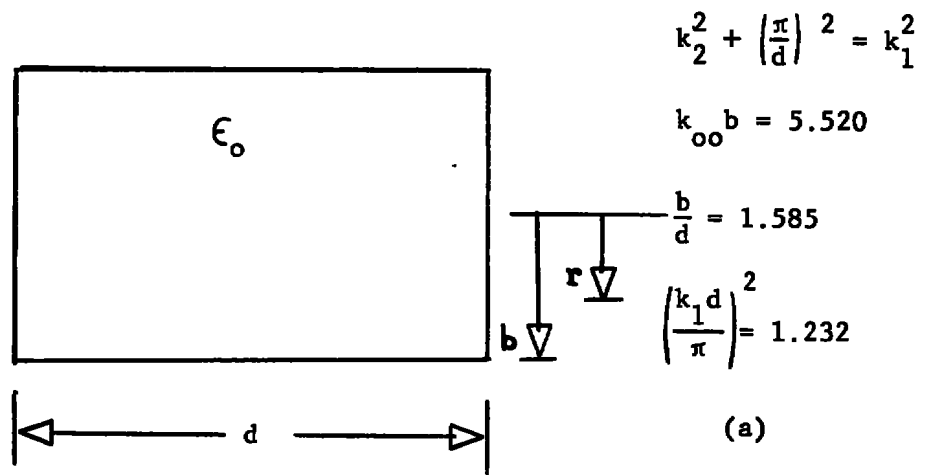
Fig. 5 Cavity Dimensions

Since circumferential modes are assumed not present, $m = o$ only. When operating TM_{020}, then $l = o$ and $p(0,2) = 5.520 = k_1 b$. When operating TM_{011}, $l = 1$ and $p(0,1) = 2.405 = k_2 b$. The numbers k_1 and k_2 are wave numbers for the respective TM_{02} and TM_{01} waveguide modes. Using this data in relation (7), one obtains the simultaneous equations

$$k_1^2 = k_{oo}^2 \qquad\qquad\qquad \text{---(8)}$$

and

$$k_2^2 + \left(\frac{m}{d}\right)^2 = k_{oo}^2 \quad (=k_1^2) \qquad . \qquad \text{---(8a)}$$

These can be solved for b and d as

$$k_{oo} b = 5.520 \qquad\qquad\qquad \text{---(9)}$$

and

$$\frac{k_1 d}{\pi} = 1.110 \qquad\qquad\qquad \text{---(9a)}$$

and, alternately,

$$\frac{b}{d} = 1.585 \qquad , \qquad\qquad\qquad \text{---(9b)}$$

in which $k_1^2 = k_{oo}^2 = \omega_o^2 \mu_o \epsilon_o$ is used to specify the frequency of operation. Since b and d are here real numbers, then the system can operate in these two modes simultaneously.

The results (9)(9a)(9b) and equation (8a) are listed in Figure (5a) for reference.

Methods of solution of the boundary value problem that would characterize the responses of a filled cavity have been discussed previously (Refs. 4, 8, 9, and 10). A variational approach, a Rayleigh-Ritz scheme such as discussed by Collin (Ref. 4), is the one used for the present cavity problem. It has the advantage that results come directly in terms of modes of interest and couplings between them. It is also helpful for expression of results by means of the very small changes in parameters (i.e., permittivity, conductance, resonant frequency) that one is concerned with here.

There are simplifying effects upon calculations which are due to radial symmetry in the wake and in the cavity modes that are chosen for measurement but, most importantly, due to the fact that the wake causes only a slight perturbation of electrical properties of air. More than this, the approach which Collin shows is special, applying just to rectangular guide, and would therefore need modification in order to try it on circular guide. The modified and simplified equations are derived below. The problem so stated yields solution fields that are approximately the correct ones, and leads to only small errors in the propagation constants and resonant frequencies that are to be evaluated. Error incurred in derivation is discussed in Appendix A.

Conditions inside the cavity during measurement are as shown in Figure (5b). The wake is assumed to be cylindrically shaped and to have a uniform dielectric constant $K \epsilon_o$ along its axial length e, and another uniform dielectric constant $M \epsilon_o$ along its axial length f.

The ratio e/f can be chosen arbitrarily, but a special rule will be shown later to specify e/f most favorably for accuracy of reading by the system.

The approach on the problem is as illustrated in Figure 6. First, the two partially filled guides are analyzed separately by the variational procedure mentioned. They will then be matched at a common planar junction. Finally, resonance will be said to occur when nodes (on either side of the junction) are separated by total length d. Frequencies found this way are the modal resonances ω_1 and ω_3 (see Figure 4.) The mode conversion frequencies ω_2, on the other hand, are not resonances in the same sense of the procedure used to find ω_1 and ω_3. However, these can be found easily enough from circuit interrelations listed in Table I.

Now let K(r) be the radial function giving relative dielectric constant, i.e.

$$K(r) = K \quad , \quad o \leqslant r < a \qquad \qquad \text{---(10)}$$
$$= 1 \quad , \quad a < r \leqslant b \quad .$$

Then for this cylindrical region the pertinent Maxwell's equations can be written

$$\nabla \times |H = j\omega \in_o K(r) |E \qquad \qquad \text{---(11)}$$

$$\nabla \times |E = -j\omega\mu_o |H \qquad \qquad \text{---(11a)}$$

$$\nabla \cdot |H = 0 \qquad \qquad \text{---(11b)}$$

$$\nabla \cdot K(r) |E = 0 \quad . \qquad \qquad \text{---(11c)}$$

$$\epsilon_o$$

$$K\epsilon_o$$

$$\epsilon_o$$

$$M\epsilon_o$$

$$\epsilon_o$$

$$K\epsilon_o \qquad M\epsilon_o$$

$$z$$

$$d$$

Fig. 6 Steps of the Resonance Calculation

In order not to labor familiar parts of the derivation process, it is noted first that only TM waves are of interest, and second that $\mathbb{E}$ and $\mathbb{H}$ can be given in terms of potentials[*] π and $\emptyset$ by

$$\mathbb{H} = j\omega\epsilon_o \nabla \times \pi \qquad \text{---(12)}$$

and, where $k_o^2 = \omega^2 \mu_o \epsilon_o$,

$$\mathbb{E} = k_o^2 \pi + \nabla \emptyset \qquad \text{---(12a)}$$

But for a factor $K(r)$, π would be an electric Hertzian potential. These two relations can be inserted into the first listed Maxwell's equation (11) to obtain the ordinarily crucial statement

$$\nabla^2 \pi + k_o^2 K(r) \pi = \nabla (\nabla \cdot \pi) - K(r) \nabla \emptyset \qquad \text{---(13)}$$

A solution of this is what is needed. Auxiliary relations will now be discussed which can simplify the steps of the calculation.

Suppose, on the right hand side of equation (13), that

$$\nabla (\nabla \cdot \pi) - \nabla \emptyset = 0 \qquad \text{---(14)}$$

This condition is usually made when specifying potential in homogeneously filled waveguide. The somewhat changed consequences of using (14) for the present partially filled guide need to be characterized. Putting (14) with (13), then π found from

$$\nabla^2 \pi + k_o^2 K(r) \pi = - \left[K(r) - 1 \right] \nabla (\nabla \cdot \pi) \qquad \text{---(15)}$$

---

[*]See Collin (Ref. 4) or Stratton (Ref. 11) for more thorough treatment of potentials.

would be the field required to solve the problem. In this case, the

associated electric field becomes

$$\mathbb{E} = k_o^2 \vec{\pi} + \nabla (\nabla \cdot \vec{\pi}) \qquad , \qquad \text{---(16)}$$

having used equation (14) to substitute for $\nabla \phi$ in equation (12a).

Continue this supposition by letting $\vec{\pi}$ take the form of a z-directed

E-wave potential

$$\vec{\pi} = \hat{z} \Psi \exp \gamma z \qquad \text{---(17)}$$

where $\Psi = \Psi(r)$ fits zero boundary conditions on the guide walls of

Figure 6, and where the propagation constant γ is a number still to be

determined. Used in equations (12) and (16), this gives for the electro-

magnetic fields the statements

$$\mathbb{H} = -j\omega \, \epsilon_o \hat{\theta} \frac{\partial \Psi}{\partial r} \exp \gamma z \qquad \text{---(18)}$$

and

$$\mathbb{E} = \left[(k_o^2 + \gamma^2) \hat{z} \Psi + \gamma \hat{r} \frac{\partial \Psi}{\partial r} \right] \exp \gamma z \qquad , \qquad \text{---(18a)}$$

where $\hat{r}$, $\hat{\theta}$, $\hat{z}$ are radial, circumferential, and axial respective unit

vectors. Plainly, with Ψ and $\frac{\partial \Psi}{\partial r}$ continuous, these $\mathbb{E}$ and $\mathbb{H}$ fields

fit correct transition conditions across the boundary between the cylindri-

cal wake and air inside the guide in Figure 6, as well also across the

planar junction between the two wake sections K and M.

This same potential $\vec{\pi}$ substituted into equation (15) gives the

two component vector statement

23

$$\left[\frac{1}{r}\frac{\partial}{\partial r}\left(r\frac{\partial \Psi}{\partial r}\right) + (k_o^2 + \gamma^2)K(r)\Psi\right]\hat{z}$$
$$+ \left[K(r) - 1\right]\gamma\frac{\partial \Psi}{\partial r}\hat{r} = 0 \qquad , \qquad \text{---}(19)$$

which is incorrect, but which is small in error even assuming the $\hat{r}$

vector component zero. The purpose of doing so is that solution of

(19) becomes simplified thereby and, moreover, that electric field

expression in terms of the potential function thereby also simplifies.

Thus the equation that needs to be solved here is

$$\frac{1}{r}\frac{\partial}{\partial r}\left(r\frac{\partial \Psi}{\partial r}\right) + K(r)(k_o^2 + \gamma^2)\Psi = 0 \qquad , \qquad \text{---}(20)$$

and the expression of $|E$ and $|H$ fields is done by formulas similar to

those used with homogeneously filled guides. The character and size

of error incurred in forgetting the r-component of $\overline{\pi}$ by using (14) is

discussed in Appendix A.

A suitable form for Ψ, for solution to (20), can be as a sum of

purely radial mode functions of the circular waveguide; i.e.,

$$\Psi = \sum_n a_n \psi_n \qquad , \qquad \text{---}(21)$$

where the a_n are amplitude coefficients and where the ψ_n are the unit

functions

$$\psi_n = \frac{\sqrt{2}}{b}\frac{J_o(k_n r)}{J_1(k_n b)} \qquad . \qquad \text{---}(22)$$

Here, J_o and J_1 are zero and first order Bessel functions. The wavenumbers

k_n are found, as specified in equation (7), such that $k_n b$ is an $n\underline{\text{th}}$ root

of the zero order Bessel function. The property that makes ψ_n a unit function is that

$$\|\psi_n\|^2 = \int_b \psi_n{}^2 \, r \, dr = 1 \quad .$$

Associated with equation (20) is the quadratic relation (Refs. 4 and 5)

$$\int_{b^-} \left| \frac{\partial \Psi}{\partial r} \right|^2 r \, dr - \int_b K(r) \left[\Gamma(\Psi)^2 + k_o^2 \right] |\Psi|^2 r \, dr = 0 \, , \qquad \text{---(23)}$$

where the function $\Gamma(\Psi)^2$ has the stationary value γ^2 whenever the correct potential Ψ is used. By being stationary, percent error in calculating $\gamma^2 + k_o^2$ this way is at worst proportional to percent mean squared error in Ψ. This is error due to approximation of fields by a finite number of modes. It is not the same as the operator approximation for (20) mentioned earlier. In fact, it is some orders less[*] an error than that in (20).

An alternate, more convenient, form for the above relation (23) can be given. Using the fact that $K(r)$ has constant values inside and outside the wake, one can write

$$\int_b \left| \frac{\partial \Psi}{\partial r} \right|^2 r \, dr - \left[\Gamma(\Psi)^2 + k_o^2 \right] \left[\int_b \Psi^2 \, r \, dr + (K-1) \int_a |\Psi|^2 r \, dr \right] = 0, \qquad \text{---(23a)}$$

where b is radius for the guide but a is radius for the wake. Assuming Ψ to have the linear form shown by relation (21), then integral terms in (23a) correspond to matrix operations (see Collin, Ref. 4) listed in

_____

[*]This can be laid to the fact that Ψ is twice differentiable, having higher modal components which are very slight.

TABLE III
OPERATOR AND QUADRATIC FORM CORRESPONDENCES

$$\Psi = \sum_n a_n \Psi_n$$

$$\int_b |\Psi|^2 rdr \quad \Longleftrightarrow \quad \begin{pmatrix} 1 & 0 \dots & \\ 0 & 1 & 0 \dots \\ \vdots & 0 & 1 \\ & \vdots & \end{pmatrix} \begin{pmatrix} a_1 \\ a_2 \\ a_3 \\ \vdots \end{pmatrix}$$

$$\int_b \left| \frac{\partial \Psi}{\partial r} \right|^2 rdr \quad \Longleftrightarrow \quad \begin{pmatrix} k_1^2 & 0 \dots & \\ 0 & k_2^2 & 0 \dots \\ \vdots & 0 & k_3^2 \\ & \vdots & \end{pmatrix} \begin{pmatrix} a_1 \\ a_2 \\ a_3 \\ \vdots \end{pmatrix}$$

$$\int_a |\Psi|^2 rdr \quad \Longleftrightarrow \quad \begin{pmatrix} \Delta_{11} & \Delta_{12} & \Delta_{13} \dots \\ \Delta_{21} & \Delta_{22} & \Delta_{23} \dots \\ \Delta_{31} & \Delta_{32} & \Delta_{33} \\ \vdots & \vdots & \end{pmatrix} \begin{pmatrix} a_1 \\ a_2 \\ a_3 \\ \vdots \end{pmatrix}$$

where $\Delta_{ij} = \Delta_{ji} = \int_a \psi_i \psi_j \, rdr$

and $\psi_i = \frac{\sqrt{2}}{b} \frac{J_o(K_i r)}{J_1(K_i b)}$

Table III.

Using these results, and assuming only the two effective modes TM_{02} (for $n = 1$) and TM_{01} (for $n = 2$), then solution of the variational problem is equivalent to solution of the matrix equation

$$\begin{pmatrix} k_1^2 - (\gamma^2 + k_o^2)\left[1 + (K-1)\Delta_{11}\right] & -(\gamma^2 + k_o^2)(K-1)\Delta_{12} \\ \\ -(\gamma^2 + k_o^2)(K-1)\Delta_{12} & k_2^2 - (\gamma^2 + k_o^2)\left[1 + (K-1)\Delta_{22}\right] \end{pmatrix} \begin{pmatrix} a_1 \\ \\ a_2 \end{pmatrix} = 0$$

---(24)

The determinant of the matrix, set to zero and solved, yields

$$\frac{2k_1^2 k_2^2}{k_o^2 + \gamma^2} = k_2^2\left[1 + (K-1)\Delta_{11}\right] + k_1^2\left[1 + (K-1)\Delta_{22}\right]$$

$$\pm \sqrt{\left\{k_2^2\left[1 + (K-1)\Delta_{11}\right] - k_1^2\left[1 + (K-1)\Delta_{22}\right]\right\}^2 + 4k_1^2 k_2^2 (K-1)^2 \Delta_{12}^2}$$

---(25)

In (25), were the propagation constants $\gamma_1 (\doteq 0)$ and $\gamma_2 (\doteq j\frac{\pi}{d})$ known, then $k_o = k_{o3}$ and $k_o = k_{o1}$ respectively would become known, and then $\omega_3^2 = (\mu_o \epsilon_o)^{-1} k_{03}^2$ and $\omega_1^2 = (\mu_o \epsilon_o)^{-1} k_{01}^2$ respectively[*] could be determined. The resonances must next be found by matching this guide (wake K) with the guide having wake M, and then closing off the ends so that it

---

[*] It turns out, as the 1-2 vs 3-1 subscripts indicate, that the π resonance (TM_{011}) has a smaller frequency change than the 0 resonance (TM_{020}). This is intuitively sensible, knowing that the waveguide is a high-pass filter whose cutoff frequency is raised by the wake. It means group velocity is higher for the cutoff TM_{02} wave, and this means a higher frequency change to reestablish resonance for the TM_{020} mode than for the TM_{011} mode.

resonates only over the length d, as suggested in Figure 6.

With very small error in approximation (even for a wake Q of 100), the γ^2 expression (25) can be put more conveniently by formulas listed in Table IV. The same adjustment worked for the second waveguide (substituting M for K) yields, with the same qualifications, results for $h_1^2 = 0$ and $h_2^2 = -\frac{\pi}{d}^2$ also shown in Table IV.

Table V shows potential field functions Ψ that can exist in the two waveguides, in terms of the basic radial mode functions ψ. It is linear combinations of these fields that one would generally use, depending on particular guide end and guide junction conditions. The coefficient matrices listed, because of the interrelations shown, are not orthogonal. However, because of small size in the cross diagonal elements, they are approximately orthogonal. These are the same coefficients needed to solve equation (24). The designations TM_{02} and TM_{01} are also only approximate since now both modes are present in each field.

Match at the junction of M and K, indicated in Figure 6, can be made in terms of transverse electric and magnetic field components derived from the Ψ potentials. Thus, from equations (18) and (18a) and from Table V,

$$\frac{1}{j\omega\epsilon_o} H_K = A_1 \frac{\partial \Psi_{1K}}{\partial r} \cosh \gamma_1 (z + e) + A_2 \frac{\partial \Psi_{2K}}{\partial r} \cosh \gamma_2 (z + e) \quad ---(26)$$

28

TABLE IV
LOADED GUIDE PROPAGATION FUNCTIONS

$\underline{TM_{02}}$

$$\frac{\gamma_1^2 + k_o^2}{k_1^2} = 1 - (K-1)\Delta_{11} + (K-1)^2\left[\Delta_{11}^2 + \left(\frac{k_1 d}{\pi}\right)^2 \Delta_{12}^2\right]$$

Relation to End
Results

$\gamma_1^2 \doteq 0$

$k_o^2 = k_{03}^2 = \omega_3^2 \mu_o \epsilon_o$

$\underline{TM_{01}}$

$$\frac{\gamma_2^2 + k_o^2}{k_2^2} = 1 - (K-1)\Delta_{22} + (K-1)^2\left[\Delta_{22}^2 - \left(\frac{k_2 d}{\pi}\right)^2 \Delta_{12}^2\right]$$

$\gamma_2^2 \doteq -\left(\frac{m}{d}\right)^2$

$k_o^2 = k_{01}^2 = \omega_1^2 \mu_o \epsilon_o$

$\underline{TM_{02}}$

$$\frac{h_1^2 + k_o^2}{k_1^2} = 1 - (M-1)\Delta_{11} + (M-1)^2\left[\Delta_{11}^2 + \left(\frac{k_1 d}{\pi}\right)^2 \Delta_{12}^2\right]$$

Relation to End
Results

$h_1^2 \doteq 0$

$k_o^2 = k_{03}^2 = \omega_3^2 \mu_o \epsilon_o$

$\underline{TM_{01}}$

$$\frac{h_2^2 + k_o^2}{k_2^2} = 1 - (M-1)\Delta_{22} + (M-1)^2\left[\Delta_{22}^2 - \left(\frac{k_2 d}{\pi}\right)^2 \Delta_{12}^2\right]$$

$h_2^2 \doteq -\left(\frac{m}{d}\right)^2$

$k_o^2 = k_{01}^2 = \omega_1^2 \mu_o \epsilon_o$

TABLE V
LOADED GUIDE POTENTIAL FIELDS

ψ_1, ψ_2 FROM TABLE III; γ, h FROM TABLE IV.

$\underline{\text{TM}_{02}}$

$\Psi_{1K} = (a_{11}\psi_1 + a_{21}\psi_2)$

$\underline{\text{TM}_{01}}$

$\Psi_{2K} = (a_{12}\psi_1 + a_{22}\psi_2)$

$$\begin{pmatrix} a_{11} & a_{12} \\ a_{21} & a_{22} \end{pmatrix}$$

$\dfrac{a_{21}}{a_{11}} \cong \left(\dfrac{k_1 d}{\pi}\right)^2 (K-1)\triangle_{12}$

$\dfrac{a_{12}}{a_{22}} \cong -\left(\dfrac{k_2 d}{\pi}\right)^2 (K-1)$

$k_1^2 a_{12} \cong -k_2^2 a_{21}$

$a_{11} = a_{22}$

$\underline{\text{TM}_{02}}$

$\Psi_{1M} = (b_{11}\psi_1 + b_{21}\psi_2)$

$\underline{\text{TM}_{01}}$

$\Psi_{2M} = (b_{12}\psi_1 + b_{22}\psi_2)$

$$\begin{pmatrix} b_{11} & b_{12} \\ b_{21} & b_{22} \end{pmatrix}$$

$\dfrac{b_{21}}{b_{11}} \cong \left(\dfrac{k_1 d}{\pi}\right)^2 (M-1)\triangle_{12}$

$\dfrac{b_{12}}{b_{22}} \cong -\left(\dfrac{k_2 d}{\alpha}\right)^2 (M-1)\triangle_{12}$

$k_1^2 b_{12} \cong -k_2^2 b_{21}$

$b_{11} = b_{22}$

30

and

$$E_{tK} = \gamma_1 A_1 \frac{\partial \Psi_{1K}}{\partial r} \text{ Sinh } \gamma_1 (z + e) + \gamma_2 A_2 \frac{\partial \Psi_{2K}}{\partial r} \text{ Sinh } \gamma_2 (z + e) \qquad ---(26a)$$

give transverse fields in the K guide, while

$$\frac{1}{j\omega \epsilon_o} H_M = B_1 \frac{\partial \Psi_{1M}}{\partial r} \text{ Cosh } h_1 (z - f) + B_2 \frac{\partial \Psi_{2M}}{\partial r} \text{ Cosh } h_2 (z - f) \qquad ---(27)$$

and

$$E_{tM} = h_1 B_1 \frac{\partial \Psi_{1M}}{\partial r} \text{ Sinh } h_1 (z - f) + h_2 B_2 \frac{\partial \Psi_{2M}}{\partial r} \text{ Sinh } h_2 (z - f) \qquad ---(27a)$$

give transverse fields in the M guide. At the junction, in these expressions, one sets $z = 0$, $H_K - H_M = 0$, and $E_{tK} - E_{tM} = 0$. In addition, since $\frac{\partial \Psi_1}{\partial r}$ and $\frac{\partial \Psi_2}{\partial r}$ are still orthogonal (and taking orthogonal components), one is led to the four equivalent statements

$$\begin{pmatrix} a_{11}\text{Cosh}\gamma_1 e & a_{12}\text{Cosh}\gamma_2 e & -b_{11}\text{Cosh }h_1 f & -b_{12}\text{Cosh }h_2 f \\ a_{21}\text{Cosh }\gamma_1 e & a_{22}\text{Cosh }\gamma_2 e & -b_{21}\text{Cosh }h_1 f & -b_{22}\text{Cosh }h_2 f \\ \gamma_1 a_{11}\text{Sinh }\gamma_1 e & \gamma_2 a_{12}\text{Sinh }\gamma_2 e & h_1 b_{11}\text{Sinh }h_1 f & h_2 b_{12}\text{Sinh }h_2 f \\ \gamma_1 a_{21}\text{Sinh }\gamma_1 e & \gamma_2 a_{22}\text{Sinh }\gamma_2 e & h_1 b_{21}\text{Sinh }h_1 f & h_2 b_{22}\text{Sinh }h_2 f \end{pmatrix} \begin{pmatrix} A_1 \\ A_2 \\ B_1 \\ B_2 \end{pmatrix} = 0$$

$$---(28)$$

put in matrix form.

31

The determinant of the (28) matrix, set to zero, yields the characteristic equation for the junction

$$\frac{h_1 h_2}{\gamma_1 \gamma_2} \frac{\tanh h_1 f}{\tanh \gamma_1 e} \frac{\tanh h_2 f}{\tanh \gamma_2 e} + 1 + \frac{h_1}{\gamma_1} \frac{\tanh h_1 f}{\tanh \gamma_1 e} + \frac{h_2}{\gamma_2} \frac{\tanh h_2 f}{\tanh \gamma_2 e}$$

$$+ (C_{11}C_{22} - 1) \left[\frac{h_1}{\gamma_1} \frac{\tanh h_1 f}{\tanh \gamma_1 e} + \frac{h_2}{\gamma_2} \frac{\tanh h_2 f}{\tanh \gamma_2 e} \right]$$

$$- C_{12}C_{21} \left[\frac{h_1}{\gamma_2} \frac{\tanh h_1 f}{\tanh \gamma_2 e} + \frac{h_2}{\gamma_1} \frac{\tanh h_2 f}{\tanh \gamma_1 e} \right] = 0 \qquad , \qquad \text{---(29)}$$

where the C multipliers are found as coefficients of the matrix

$$\begin{pmatrix} C_{11} & C_{12} \\ C_{21} & C_{22} \end{pmatrix} = \frac{1}{a_{11}a_{22} - a_{12}a_{21}} \begin{pmatrix} a_{22} & -a_{12} \\ -a_{21} & a_{11} \end{pmatrix} \begin{pmatrix} b_{11} & b_{12} \\ b_{21} & b_{22} \end{pmatrix}$$

$$= \frac{1}{a_{11}a_{22} - a_{12}a_{21}} \begin{pmatrix} a_{22}b_{11} - a_{12}b_{21} & a_{22}b_{12} - a_{12}b_{22} \\ -a_{21}b_{11} + a_{11}b_{21} & -a_{21}b_{12} + a_{11}b_{22} \end{pmatrix} .$$

$$\text{---(30)}$$

By using (30) and results in Tables IV and V, one can show the last two bracketed terms in (29) to have value proportional to $(C_{12}C_{21})^2$. This is by some orders smaller than previously mentioned errors. Ignoring these terms, then the junction characteristic equation (29) can be written in the much simplified form

$$\left[\frac{h_1}{\gamma_1} \frac{\tanh h_1 f}{\tanh \gamma_1 e} + 1 \right] \left[\frac{h_2}{\gamma_2} \frac{\tanh h_2 f}{\tanh \gamma_2 e} + 1 \right] = 0 \qquad . \qquad \text{---(31)}$$

If one takes advantage of the fact that propagation constants of the loaded guide are but slightly changed from those of the empty guide,

then (31) can be rewritten

$$\left[h_1^2 f + \gamma_1^2 e\right]\left\{\left[h_2^2 + \left(\tfrac{m}{d}\right)^2\right] f + \left[\gamma_2^2 + \left(\tfrac{\pi}{d}\right)^2\right]e\right\} = 0 \qquad ---(31a)$$

These last two expressions of the junction characteristic

equation point to an interesting property of the cavity: namely, that

the γ_1 and h_1 modes affect only each other, as also do the γ_2 and h_2

modes. The chief perturbing influence on behaviour of the cavity, in

other words, is the wake ionization in front relative to ionization

behind. Qualitatively, this is good. It suggests it is only a mild

assumption -- even at high front to back ionization ratios -- to hold

that the wake can be characterized by a sudden change in its dielectric

constant. It is not to say there should not be such coupling, but without

coupling there is less that needs explaining. The matter is argued

briefly as follows.

Use of equation (31) is equivalent to the assumptions

$$a_{12} = a_{21} = b_{12} = b_{21} = 0 \text{ and } a_{11} = a_{22} = b_{11} = b_{22} = 1$$

in the statement of equation (28). In this case, that homogeneous ex-

pression can be rewritten as

$$\begin{pmatrix} \cosh \gamma_1 e & 0 & -\cosh h_1 f & 0 \\ 0 & \cosh \gamma_2 e & 0 & -\cosh h_2 f \\ \gamma_1 \sinh \gamma_1 e & 0 & h_1 \sinh h_1 f & 0 \\ 0 & \gamma_2 \sinh \gamma_2 e & 0 & h_2 \sinh h_2 f \end{pmatrix} \begin{pmatrix} A_1 \\ A_2 \\ B_1 \\ B_2 \end{pmatrix} = 0 .$$

$$---(32)$$

33

It is plain that solution vectors for (32) must look either

$$
\text{like} \quad \begin{pmatrix} 1 \\ 0 \\ 1 \\ 0 \end{pmatrix} \text{or else like} \quad \begin{pmatrix} 0 \\ 1 \\ 0 \\ 1 \end{pmatrix} . \qquad \text{---(33)}
$$

There are no other solution vectors for (32). These forms (33) agree with the qualitative suggestion of cavity behaviour just made.

The junction characteristic equation (31a), substituting γ and h expressions from Table IV, can be solved for k_{01} and k_{03}. For $\gamma_1 h_1$, one sets $k_o = k_{03}$ to solve. For $\gamma_2 h_2$, one sets $k_o = k_{01}$ to solve. Results (with negligible additional error) are listed in Table VI in several forms. The relations $k_1^2 = k_{oo}^2 = \omega_o^2 \mu_o \epsilon_o$, $k_{01}^2 = \omega_1^2 \mu_o \epsilon_o$, and $k_{03}^2 = \omega_3^2 \mu_o \epsilon_o$ were also used for the expressions in Table VI. It is interesting to note here that the number

$$
\overline{K-1} = \frac{e}{d}(K-1) + \frac{f}{d}(M-1) \qquad \text{---(34)}
$$

is mean susceptibility while the number

$$
\overline{(K-1)^2} = \frac{e}{d}(K-1)^2 + \frac{f}{d}(M-1)^2 \qquad \text{---(35)}
$$

is only a formal mean square susceptibility. That is, in the first place, (35) gives information derived solely from the mean value. In the second place, both (34) and (35) retain complex number information about wake susceptibility. Thus, while the single mode cavity is well known to give

34

TABLE VI
CAVITY WAVENUMBERS AND RESONANCES

$$\frac{\omega_1^2 - \omega_o^2}{\omega_o^2} = \frac{k_{01}^2 - k_1^2}{k_1^2} = - \overline{(K-1)}\left(\frac{k_2}{k_1}\right)^2 \Delta_{22} + \overline{(K-1)^2}\left(\frac{k_2}{k_1}\right)^2\left[\Delta_{22}^2 - \left(\frac{k_2 d}{\pi}\right)^2 \Delta_{12}^2\right] \underline{\text{Low}}$$

$$\frac{\omega_3^2 - \omega_o^2}{\omega_o^2} = \frac{k_{03}^2 - k_1^2}{k_1^2} = - \overline{(K-1)}\Delta_{11} + \overline{(K-1)^2}\left[\Delta_{11}^2 + \left(\frac{k_1 d}{\pi}\right)^2 \Delta_{12}^2\right] \qquad \underline{\text{High}}$$

$$\frac{\omega_3^2 - \omega_1^2}{\omega_o^2} = \frac{k_{03}^2 - k_{01}^2}{k_1^2} = -\overline{(K-1)}\left[\Delta_{11} - \left(\frac{k_2}{k_1}\right)^2 \Delta_{22}\right]$$

$$+ \overline{(K-1)^2}\left[\Delta_{11}^2 - \left(\frac{k_2}{k_1}\right)^2 \Delta_{22}^2 + \frac{k_1^4 + k_2^4}{k_1^4}\left(\frac{k_2 d}{\pi}\right)^2 \Delta_{12}^2\right]$$

$$\frac{k_{01}^2 - k_1^2}{k_2^2} = - \overline{(K-1)}\Delta_{22} + \overline{(K-1)^2}\left[\Delta_{22}^2 - \left(\frac{k_2 d}{\pi}\right)^2 \Delta_{12}^2\right]$$

$$\overline{K-1} = \frac{e}{d}(K-1) + \frac{f}{d}(M-1) \text{ Mean Susceptibility}$$

$$\overline{(K-1)^2} = \frac{e}{d}(K-1)^2 + \frac{f}{d}(M-1)^2 \underline{\text{Formal}} \text{ Mean Square Susceptibility}$$

an averaged result, the two moded cavity is here seen to give both an averaged and a kind of averaged square result. This property, it will be shown later, provides help toward improvement of accuracy of system measurements and toward an increase in information available from the system.

There is error in the assumption, for results in Table VI, that K and M can be complex numbers. However, it is small error -- of the same type and amount as that in the approximation of equation (19) by equation (20) -- and therefore accounted negligible. When K and M are complex, then the frequencies ω_o, ω_1, and ω_3 are also complex. Indeed, say such that

$$j\omega \Longleftrightarrow s = \sigma + j\omega \qquad \text{---(36)}$$

indicates the replacement necessary for these respective frequencies.

Now consider the effect on Table VI formulas. One has it, for example when $j\omega_1 \longrightarrow s_1 = \sigma_1 + j\omega_1$ and $j\omega_o \longrightarrow s_o = j\omega_o$, that

$$\frac{\omega_1^2 - \omega_o^2}{\omega_o^2} \Longleftrightarrow \frac{s_1^2 - s_o^2}{s_o^2}$$

$$= \frac{s_1 - s_o}{s_o} \frac{s_1 + s_o}{s_o}$$

$$= \frac{\sigma_1 + j(\omega_1 - \omega_o)}{j\omega_o} \frac{s_1 + s_o}{s_o}$$

$$= \frac{\sigma_1}{j\omega_o} \frac{s_1 + s_o}{s_o} + \frac{\omega_1 - \omega_o}{\omega_o} \frac{s_1 + s_o}{s_o}$$

36

$$\pm \frac{\sigma_1}{j\omega_o} \left[2 + \frac{\omega_1 - \omega_o}{\omega_o} \frac{\omega_1 + \omega_o}{\omega_o} \right]$$

$$= \frac{\omega_1^2 - \omega_o^2}{\omega_o^2} + \frac{2\sigma_1}{j\omega_o} \qquad . \qquad \text{---(37)}$$

The approximation is a good one, since it falls upon frequency differences and not upon absolute frequencies. The same treatment shows also that

$$\frac{\omega_3^2 - \omega_o^2}{\omega_o^2} \longrightarrow \frac{s_3^2 - s_o^2}{s_o^2}$$

$$\doteq \frac{\omega_3^2 - \omega_o^2}{\omega_o^2} + \frac{2\sigma_3}{j\omega_o} \qquad , \qquad \text{---(38)}$$

and that

$$\frac{\omega_3^2 - \omega_1^2}{\omega_o^2} \longrightarrow \frac{s_3^2 - s_1^2}{s_o^2}$$

$$\doteq \frac{\omega_3^2 - \omega_1^2}{\omega_o^2} + \frac{2(\sigma_3 - \sigma_1)}{j\omega_o} \qquad . \qquad \text{---(39)}$$

By comparing these frequency and decay rate expressions (37) (38) (39) with equivalent ones in Table II and in Table VI, one sees there are formulas now to relate cavity equivalent circuit measurements with cavity electromagnetic field calculations. These are listed in Table VII. One can notice these expressions are linear in the susceptibility averages, and so solve for them in terms of known measurable and calculable quantities of the system, as also listed. The last formula listed is a design

TABLE VII
CIRCUIT MEASUREMENTS RELATED TO MODAL CALCULATIONS

$$\left(\frac{k_1}{k_2}\right)^2 \left[\frac{L_o}{L_1} + j\,\frac{g_1}{Q_1}\right] = -\,\overline{(K-1)}\triangle_{22} + \overline{(K-1)^2}\left[\triangle_{22}^2 - \left(\frac{k_2 d}{\pi}\right)^2 \triangle_{12}^2\right]$$

$$\left[\frac{L_o}{L_1} + j\,\frac{g_1}{Q_1}\right] + \left(1 + \frac{1}{q}\right)\left[\frac{L_o}{L_2} + j\,\frac{g_2}{Q_2}\right] = -\,\overline{(K-1)}\triangle_{11} + \overline{(K-1)^2}\left[\triangle_{11}^2 + \left(\frac{k_1 d}{\pi}\right)^2 \triangle_{12}^2\right]$$

$$(1 + \frac{1}{q})\left[\frac{L_o}{L_2} + j\,\frac{g_2}{Q_1}\right] = -\overline{(K-1)}\left[\triangle_{11} - \left(\frac{k_2}{k_1}\right)^2 \triangle_{22}\right]$$

$$+ \,\overline{(K-1)^2}\left\{\triangle_{11}^2 - \left(\frac{k_2}{k_1}\right)^2 \triangle_{22}^2 + \left[1 + \left(\frac{k_2}{k_1}\right)^4\right]\left(\frac{k_1 d}{\pi}\right)^2 \triangle_{12}^2\right\}$$

Linear Equations Solved Using $\triangle_{12}^2 \stackrel{\doteq}{=} \triangle_{11}\triangle_{22}$.

$$\overline{K-1} = \frac{\left(\frac{\pi}{k_2 d}\right)^2}{\triangle_{22}}\frac{1 - \left(\frac{k_1}{k_2}\right)^2 \frac{\triangle_{11}}{\triangle_{22}}}{1 + \left(\frac{k_1}{k_2}\right)^2 \frac{\triangle_{11}}{\triangle_{22}}}\left[\left(1 - \frac{\left[\left(\frac{k_1}{k_2}\right)^2 + \left(\frac{k_2}{k_1}\right)^2\right]\left(\frac{k_1 d}{\pi}\right)^2 \frac{\triangle_{11}}{\triangle_{22}}}{1 - \left(\frac{k_1}{k_2}\right)^2 \frac{\triangle_{11}}{\triangle_{22}}}\right)\left(\frac{L_o}{L_1} + j\,\frac{g_1}{Q_1}\right)\right.$$

$$\left. + \frac{1 - \left(\frac{k_2 d}{\pi}\right)^2 \frac{\triangle_{11}}{\triangle_{22}}}{1 - \left(\frac{k_1}{k_2}\right)^2 \frac{\triangle_{11}}{\triangle_{22}}}\left(1 + \frac{1}{q}\right)\left(\frac{L_o}{L_2} + j\,\frac{g_2}{Q_1}\right)\right]$$

$$\overline{(K-1)^2} = \frac{\left(\frac{\pi}{k_2 d}\right)^2}{\triangle_{11}\triangle_{22}}\frac{1 - \left(\frac{k_1}{k_2}\right)^2 \frac{\triangle_{11}}{\triangle_{22}}}{1 + \left(\frac{k_1}{k_2}\right)^2 \frac{\triangle_{11}}{\triangle_{22}}}\left[\left(\frac{L_o}{L_1} + j\,\frac{g_1}{Q_1}\right) + \frac{\left(1 + \frac{1}{q}\right)}{1 - \left(\frac{k_1}{k_2}\right)^2 \frac{\triangle_{11}}{\triangle_{22}}}\left(\frac{L_o}{L_2} + j\,\frac{g_2}{Q_1}\right)\right]$$

Continued next page

TABLE VII (Concluded)

$$\Delta_{11} \cong \left(\frac{a}{b} \frac{1}{J_1(k_1b)}\right)^2 \quad , \quad \Delta_{22} \cong \left(\frac{a}{b} \frac{1}{J_1(k_2b)}\right)^2 , \left(\frac{k_1}{k_2}\right)^2 \frac{\Delta_{11}}{\Delta_{22}} \cong \left(\frac{k_1J_1(k_2b)}{k_2J_1(k_1b)}\right)^2$$

$$k_1b = 5.5201, \quad J_1(k_1b) = 0.3403, \quad k_2b = 2.4048, \quad J_1(k_2b) = -0.5191$$

$$\left(\frac{k_1J_1(k_2b)}{k_2J_1(k_1b)}\right)^2 - 1 \cong \left(1 + \frac{k_1Q_1}{k_2Q_2}\right) \frac{\frac{L_o}{L_2} + j\frac{g_2}{Q_1}}{\frac{L_o}{L_1} + j\frac{g_1}{Q_1}} \quad \text{Design Figure of Merit}$$

figure of merit for the system. It is derived assuming $\overline{K-1}$ small and $\overline{(K-1)}^2$ negligible. What it asks is that the design be done so that the two measured admittances be roughly the same order of size. Failing that, one could need to inquire into the accuracy of measurement of them. Table VII gives the final results of this section. There remains just the special choice of e/f cavity axial division to give and to interpret.

SECTION IV
OPTIMIZED CAVITY MEASUREMENT

The formal averages in Table VII, once a ratio $\frac{e}{f}$ is specified, can let one calculate an M in the f section and a K in the e section of the cavity (i.e., by solving equations (34) and (35)). However, every choice $\frac{e}{f}$ lets some corresponding K and M be calculated. One could ask whether there is not some optimum $\frac{e}{f}$ choice which should be made for a preferred K and M pair; in particular, to be done without requiring additional measured data. A preferred $\frac{e}{f}$ ratio can be that which locates the junction where actual electric susceptibility is the same as measured average $\overline{K-1}$. This is all the more so a good choice because it also means that K-1 and M-1 are actual averages over the respective e and f cavity sections. Most importantly, this $\frac{e}{f}$ marks the wake at a particular distance behind the model such that subsequent graphs are then precisely tied to model location.

A positive choice can be made. The question raised is perhaps not such a simple one as the approach in answer to it reflects. Nonetheless, it is a step in the right direction. Indeed the suggestion that is made is such as should be applied to all data. The matter is a physical one. Essentially, it attempts to make the junction (the sudden susceptibility change) appear as unobtrusive as possible. In doing so, it matches the physical character of the wake at the same time. One result is to allow higher M-1 to K-1 ratios to be read than

for the case $e = f = \frac{d}{2}$, but this is a property of any move away from a half-half split in cavity axial length.

The matter is stated as follows. Consider two slices of the wake as shown in Figure 7 (or even smaller constant volume elements). The energy difference between the Δe and Δf sections can be much larger at the junction than if the slices were moved together anywhere else along the wake. By comparison, if this were the real wake without junctions, differential energy between the slices would still vary as the pair were moved about, but variation would be by a second order of slice size -- not by a first order. One can say that large energy differential at the junction corresponds to first order error which should be reduced.

The energy in the wake is almost entirely electric. In the slices, it is proportional to $(K-1)\Delta e$ in the e section, and to $(M-1)\Delta f$ in the f section. Proportionality is the same for both sides since both sides have approximately the same field strengths. Therefore, the difference

$$(K-1)\Delta e - (M-1)\Delta f = \Delta \mathcal{E} \qquad \text{---(40)}$$

is the thing to minimize. Now equations (34) and (35) can be solved to give

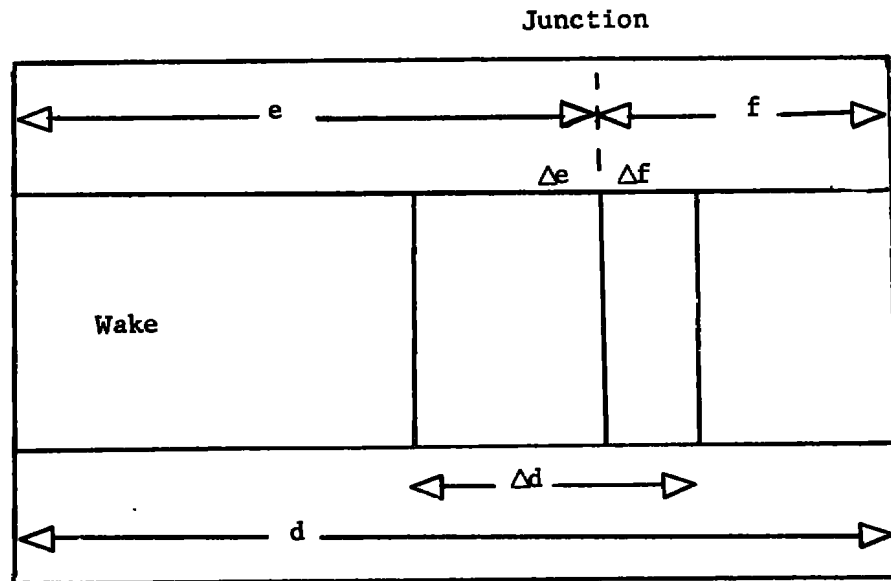$$K-1 = \overline{K-1} \sqrt{\frac{e}{f}} \sqrt{(K-1)^2 - (\overline{K-1})^2} \qquad \text{---(41)}$$

42

Junction

Fig. 7 Volume Element in Differential Energy Test

and

$$M-1 = \overline{K-1} + \sqrt{\frac{f}{e}} \sqrt{(K-1)^2 - (\overline{K-1})^2} \quad . \qquad\qquad ---(42)$$

Substituting into relation (40) gives

$$\Delta\mathcal{E} = \overline{K-1} \ \Delta d - \left(\Delta e \sqrt{\frac{e}{f}} + \Delta f \sqrt{\frac{f}{e}}\right) \sqrt{(K-1)^2 - (\overline{K-1})^2} \quad , \qquad ---(43)$$

where $\Delta e + \Delta f = \Delta d$ is constant. Differentiating $\Delta\mathcal{E}$ with respect to $\frac{e}{f}$ gives the minimizing condition

$$\frac{\Delta e}{\Delta f} = \frac{e}{f} \quad . \qquad\qquad ---(44)$$

This result put into (40) yields finally the junction location condition

$$(K-1)e = (M-1)f \quad . \qquad\qquad ---(45)$$

The energy that would pour through the junction because of sudden susceptibility change is thereby reduced at this position. Looked at from another point of view, condition (45) holds that there is the same weight of ionized material in the forward part as in the rearward part of the cavity.

The equations (45)(42) and (41) (or (45)(34) and (35)) can be solved to put e and f explicitly in terms of measurements, and are all collected and placed in Table VIII. These results constitute the end point of the measurement procedure discussed heretofore.

TABLE VIII
OPTIMIZED MEASUREMENT RELATIONS

$$K-1 = \overline{K-1}\left[1 - \left(1 + \sqrt{1 - A^2}\right)\sqrt{B^2 - 1}\right]$$

$$M-1 = \overline{K-1}\left[1 + \left(1 - \sqrt{1 - A^2}\right)\sqrt{B^2 - 1}\right]$$

$$\frac{e}{d} = \frac{1}{2}\left(1 + \sqrt{1 - A^2}\right)$$

$$\frac{f}{d} = \frac{1}{2}\left(1 - \sqrt{1 - A^2}\right)$$

$$\left.\begin{array}{l} \dfrac{e}{f} = \dfrac{M-1}{K-1} = \left(B + \sqrt{B^2 - 1}\right)^2 \\[3em] \dfrac{f}{e} = \dfrac{K-1}{M-1} = \left(B - \sqrt{B^2 - 1}\right)^2 \end{array}\right\} \quad \text{Junction Location Condition}$$

where $A^2 = B^{-2} = \dfrac{(\overline{K-1})^2}{(K-1)^2}$ and where $(\overline{K-1})$ and $\overline{(K-1)^2}$ are found from

measurements given in Table VII.

REFERENCES

1. Berk, A. D., "Variational Principles for Electromagnetic Resonators and Waveguides," IRE Trans., vol AP-4, pp 104-111, April, 1956.

2. Bullis, R. H., "Investigation to Determine Collision Frequencies of Typical Re-entry Wake Contaminants, United Aircraft Corporation UACRL F-920440-6, April, 1967.

3. Chodorow, M. and Susskind, C., Fundamentals of Microwave Electronics, McGraw-Hill Book Company, Inc., New York, 1964.

4. Collin, R. E., Field Theory of Guided Waves, McGraw-Hill Book Co., Inc., New York, 1960.

5. Courant, R., and Hilbert, D., Methods of Mathematical Physics, Vol. I, Interscience Publishers, New York, 1953.

6. Edsall, R. H., Bisbing, P. E., and Numerich, F. H., "Analysis of Communications Attenuation Data for Blunt and Slender Re-entry Vehicles in Flight," Proceedings of the Third Symposium on the Plasma Sheath-Plasma Electromagnetics of Hypersonic Flight, Vol. I, May 1967, pp. 4-5, unclassified Abstract, Classified report.

7. Hord, W. E. and Rosenbaum, F. J., "Approximation Technique for dielectric Loaded Waveguides," IEEE Trans. Microwave Theory and Techniques, vol. MTT-16 pp. 228-240, April, 1968.

8. Kornegay, Wade M., "Electron Density Decay in Wakes." AIAA Journal, Vol. 3, No. 10, October, 1965, pp. 1819-1823.

9. Laug, M. and Clavelin, P., "Sondage Des Plasmas Par Des Mesures D'Impedance (Probing of Plasmas by Impedance Measurements)," Proceedings of First International Congress on Instrumentation in Aerospace Simulation Facilities, Paris, France, September 28-29, 1964, pp. 6-1--6-8, Intercom, 1964.

10. Slater, J. C., <u>Microwave Electronics</u>, D. Van Nostrand Company, Inc., Princeton, New Jersey, 1950.

11. Stratton, J. A., <u>Electromagnetic Theory</u>, McGraw-Hill Book Company, Inc., New York, 1941.

APPENDIX A
ERROR IN APPROXIMATING THE WAVE EQUATION

The manner by which error is considered here rests on the

facts that the loaded guide is but a slightly perturbed empty guide,

and that all field components are but slightly perturbed by about

the same proportional amount from empty guide fields. In this view

more particularly, the correction field is not just small but is at

the same time smooth. The modal amplitude coefficients decrease rapidly.

Therefore, even a field approximated by one or two modes can serve for

a test of the wave operator in (15) without causing serious effects due

to the finite mode approximation. It can be assumed because of this

that loaded guide operators work on fields very nearly the same as

those of the empty guide, and yield valid estimates for error due to

operator approximations.

The following property of stationary eigenvalues λ of a symmetric

operator $\underline{A}$ is useful. The error $\Delta\lambda$ is of the second order and can be

written

$$\Delta\lambda = \frac{(y, \underline{A}\, y) - \lambda\|y\|^2}{\|x + y\|^2} \quad , \quad \text{---(46)}$$

where x is an exact field, $x + y$ an approximate field, and y the error

component. If $\underline{A}$ has an eigenvalue λ' very close to λ, and if y can be

held to the corresponding eigenvector for λ', then the error (46) can be

rewritten as

$$\Delta\lambda = (\lambda' - \lambda) \frac{\|y\|^2}{\|x + y\|^2} \quad , \qquad \qquad \text{---(47)}$$

thereby bounding corrections put on λ. In particular, this is good because only some lowest eigenvalues of $\underline{A}$ have interest here, and these are well enough separated between themselves and from higher characteristic values.

Now the potential π that solves equation (15) can more generally have the form

$$\pi = \left[\hat{r}\frac{\partial\Phi}{\partial r} + \hat{z}\Psi\right]\exp(\gamma z) \quad , \qquad \qquad \text{---(48)}$$

where Φ and Ψ are approximately proportional. In the empty guide as in the completely filled guide, Φ and Ψ can be identical. If (48) is inserted into the vector equation (15), then the pair of scalar equations

$$\frac{1}{r}\frac{\partial}{\partial r}\left(r\frac{\partial\Psi}{\partial r}\right) + K(r)(\gamma^2 + k_o^2)\Psi + (K(r) - 1)\gamma\frac{1}{r}\frac{\partial}{\partial r}\left(r\frac{\partial\Phi}{\partial r}\right) = 0 \text{---(49)}$$

and

$$(K(r) - 1)\gamma\frac{\partial\Psi}{\partial r} + K(r)\frac{1}{r}\frac{\partial}{\partial r}\left(r\frac{\partial^2\Phi}{\partial r^2} + \left[\gamma^2 + K(r)k_o^2\right]\frac{\partial\Phi}{\partial r}\right) = 0 \qquad \text{---(49a)}$$

can be put down. If it is taken that $\Psi \doteq x\psi$ and $\Phi \doteq y\psi$, where ψ is a unit Bessel function from Table III and where corrections to Ψ and Φ are small and nearly proportional, then the equations (49) and (49a) can be put in the equivalent matrix form

49

$$\begin{pmatrix} -k^2 + (\gamma^2 + k_o^2)\left[1 + (K-1)\Delta\right] & -(K-1)\gamma k\Delta \\ (K-1)\gamma k\Delta & (-k^2 + k_o^2)\left[1 + (K-1)\Delta\right] + \gamma^2 \end{pmatrix}\begin{pmatrix} x \\ y \end{pmatrix} = 0.$$

---(50)

Here, k and Δ are k_1 and Δ_{11} for the TM_{02} mode and k_2 and Δ_{22} for the TM_{01} mode. It will not be necessary to specify k and Δ to correspond to either one or the other mode. The same treatment would serve for each of them.

The determinant for (50), set to zero and solved, yields the two propagation constants

$$\gamma(\Phi)^2 = -k_o^2 + k^2 - k_o^2(K-1)\Delta$$

---(51)

and

$$\gamma(\Psi)^2 = -k_o^2 + k^2 \quad ,$$

---(51a)

associated with the Φ and Ψ potentials respectively; both very nearly zero. This is in contrast to what happens with loadings for travelling wave tubes. There, one needs to separate two modes so as to be able to use the slower wave (Chodorow and Susskind, Ref. 3). Here, two modes are needed in order to determine a maximum phase change for the system under loading. The phase change can be determined from

$$\gamma^2 = \gamma(\Psi)^2 + \gamma(\Phi)^2$$

$$= -k_o^2 + k^2 + k^2(1-K)\Delta \quad ,$$

---(52)

for which the following three comments apply. Firstly, both Φ and Ψ potentials contribute to the split and shift of resonance discussed

in Sections II and III. Secondly, the result (52) is derived by working through the junction matching procedure given in Section III. Thirdly, the approximation (15) holds even giving more modal components to the potentials Φ and Ψ. The result (52) is thus taken for a lower bound on values γ^2.

For $\gamma(\Phi)^2$ and $\gamma(\Psi)^2$ in (51)(51a), one finds from (50) either

$$\left|\frac{y}{x}\right| \text{ or } \left|\frac{x}{y}\right| = \sqrt{(K-1)\Delta} \qquad , \qquad \text{---(53)}$$

depending on the potential mode figured. This means that π, in terms of its component amplitudes can look like either the vector

$$\hat{y}\sqrt{(K-1)\Delta} \quad + \hat{z} \qquad \text{---(54)}$$

for $\gamma(\Psi)$, or else the vector

$$\hat{r} + \hat{z}\sqrt{(K-1)\Delta} \qquad \text{---(54a)}$$

for $\gamma(\Phi)$. The vectors (54) and (54a) would have the same magnitude error, were the smaller component overlooked in each of them. However, it is the Ψ potential which is the more useful one. The reason for $\gamma(\Psi)^2$ so small in (51a) is due to coupling between Ψ and Φ in (50) and in (49)(49a). Without coupling, the solution to (49) will yield a propagation constant bounded by (52) and by an upper bound to be discussed now.

Equations (49)(49a), without arguing this,[*] can be put suitably

to test the vector (54) in the error criterion (47). Doing so, letting

λ be a value of $\dfrac{k_o^2 + \gamma^2}{k^2} - 1$ and $\Delta\lambda$ the error in this quantity, then

$$\Delta\lambda \approx \left|\lambda' - \lambda\right| \frac{\left|(K-1)\Delta\right|}{1 + \left|(K-1)\Delta\right|}$$

$$\approx \left|\lambda' - \lambda\right|\left|(K-1)\Delta\right| \qquad\qquad \text{---(55)}$$

requires just an estimate of the eigenvalue separation $\left|\lambda' - \lambda\right|$. A

lower bound, already given by (52), an upper bound is needed.

This is shown from consideration of $\dfrac{\gamma^2 + k_o^2}{k^2} - 1$ found from three

possible wave operator approximations. The three,

$$\nabla_t^2 + K(r)(\gamma^2 + k_o^2) \qquad , \qquad\qquad \text{---(56)}$$

$$\nabla_t^2 + \gamma^2 + K(r)k_o^2 \qquad , \qquad\qquad \text{---(56a)}$$

$$K(r)\nabla_t^2 + \gamma^2 + K(r)k_o^2 \qquad , \qquad\qquad \text{---(56b)}$$

all working on radial functions, are not hard to interpret. All are

correct for an empty guide. Only (56a) is correct for a filled guide. A

comparison of their effects on λ is shown in Figure 8, where the scale

$(K-1)\Delta$ is proportional to $\left|\dfrac{a}{b}\right|^2$ only when $\left|\dfrac{a}{b}\right|^2$ is small.
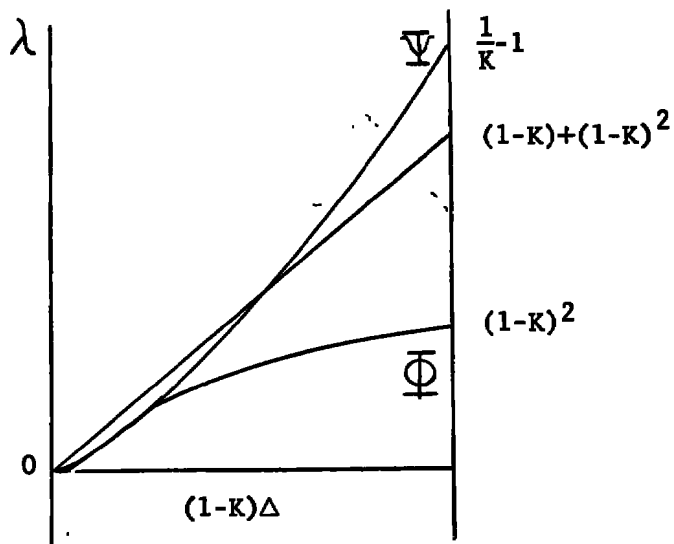
The operator (56b) corresponding to the uncoupled ϕ potential, yields

λ always too small. The operator (56), corresponding to the uncoupled ψ

---

[*]These are rearrangements using operator formalisms.

Worst Case -

At Measurement
Frequency ω_o

λ

$\overline{\Psi}$

$\frac{1}{K}-1$

$1-K$

$\underline{\Phi}$

0

$(1-K)\Delta$
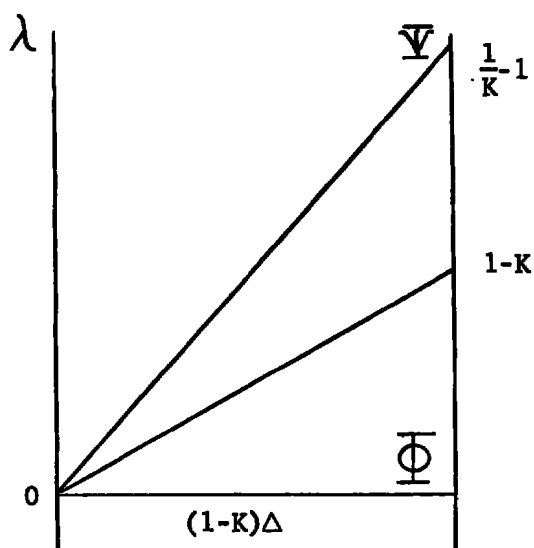
Next Worse Case -

At Cavity Resonance

λ

$\overline{\Psi}$

$\frac{1}{K}-1$

$(1-K)+(1-K)^2$

$(1-K)^2$

$\underline{\Phi}$

0

$(1-K)\Delta$

Best Case -

At Cavity Resonance

Illustration of

$\overline{\Psi}$ - $\underline{\Phi}$ Coupling

λ

$\overline{\Psi}$

$\frac{1}{K}-1$

$(1-K)+(1-K)^2$
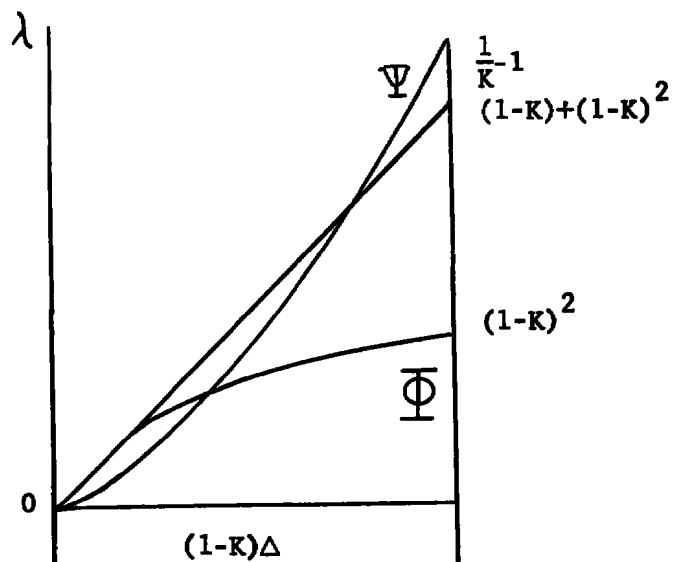
$(1-K)^2$

$\underline{\Phi}$

0

$(1-K)\Delta$

Fig. 8 Bounds of Approximated Operator

potential, provides a worst case upper bound on λ at the measurement frequency ω_o. The operator (56a) provides a next worst case upper bound on λ for small $\left(\dfrac{a}{b}\right)^2$ at the frequency of loaded cavity resonance. The best case curves, also at loaded cavity resonance, are not used for the bound evaluation but are meant to illustrate the effect on λ of coupling the ϕ and ψ potentials as in equations (49) (49a). From equation (52), and from the best case curves, λ would be the sum of the ψ and ϕ curves.

From the worst case curves, the upper bound for λ yields

$$\Delta\lambda \cong \left| \frac{(K-1)^3 \Delta^2}{K} \right| \qquad , \qquad\qquad\qquad\qquad \text{---}(57)$$

which can be suitable for larger wake diameters $\left(\dfrac{a}{b}\right)^2$ than in the present case. For the assumed present wake size (small $\left(\dfrac{a}{b}\right)^2$), from the next worst case curves, the upper bound for λ yields

$$\Delta\lambda \cong \left| (K-1)\Delta \right|^3 \qquad\qquad\qquad\qquad\qquad \text{---}(58)$$

The error estimate (58) implies, if equation (15) is used to represent the loaded cavity, and if a wake with Q (= $|K - 1|^{-1}\Delta^{-1}$) about 100 is measured for example (enough to short the system out), then calculation error could limit the determination of wake average location to an interval of 0.1 inch out of a 10 inch long cavity.

DOCUMENT CONTROL DATA - R & D

(Security classification of title, body of abstract and indexing annotation must be entered when the overall report is classified)

1. ORIGINATING ACTIVITY *(Corporate author)*	2a. REPORT SECURITY CLASSIFICATION
The University of Tennessee Electrical Engineering Department Knoxville, Tennessee	UNCLASSIFIED
	2b. GROUP N/A

3. REPORT TITLE

A MULTIMODED CAVITY PROBE TO PROVIDE HIGH SPATIAL RESOLUTION OF WAKE TRAIL IONIZATION MEASUREMENT

4. DESCRIPTIVE NOTES *(Type of report and inclusive dates)*

Final Report   March 1967 to March 1968

5. AUTHOR(S) *(First name, middle initial, last name)*

D. Rosenberg, The University of Tennessee

6. REPORT DATE	7a. TOTAL NO. OF PAGES	7b. NO. OF REFS
February 1969	61	11

8a. CONTRACT OR GRANT NO. F40600-67-C-0012	9a. ORIGINATOR'S REPORT NUMBER(S)
b. PROJECT NO. 8952	AEDC-TR-69-32
c. Task 01	9b. OTHER REPORT NO(S) *(Any other numbers that may be assigned this report)*
d. Program Element 62201F	N/A

10. DISTRIBUTION STATEMENT

This document has been approved for public release and sale; its distribution is unlimited.

11. SUPPLEMENTARY NOTES	12. SPONSORING MILITARY ACTIVITY
Available in DDC.	Arnold Engineering Development Center, Air Force Systems Command, Arnold AF Station, Tenn. 37389

13. ABSTRACT

This report discusses properties and use of a highly resolving r.f. cavity probe system for wake trails in hypervelocity model ranges. Data are taken from two distinct modes of the system and yield electric susceptance at an average axial position inside the cavity. This is important in wake trail study, since it ties together a wake electrical measurement with distance behind a hypervelocity model.

DD FORM 1473

14. KEY WORDS	LINK A		LINK B		LINK C	
	ROLE	WT	ROLE	WT	ROLE	WT
1 cavity resonators						
2 wakes -- Ionization						
hypervelocity flow						

3. Ionization - Measurements

4 cavity probes.

AFR
Arnold AFS Tenn